ChemComm

Cite this: *Chem. Commun.*, 2012, **48**, 7934–7936

www.rsc.org/chemcomm

COMMUNICATION

Cerium oxide nanoparticle-mediated self-assembly of hybrid supramolecular hydrogels†

Avinash J. Patil,* Ravinash Krishna Kumar, Nicholas J. Barron and Stephen Mann*

Received 9th May 2012, Accepted 14th June 2012
DOI: 10.1039/c2cc33351a

Hybrid supramolecular hydrogels are prepared by non-enzymatic dephosphorylation of *N*-fluorenylmethyloxycarbonyl tyrosine-(*O*)-phosphate (FMOC-Tyr-P) using catalytic cerium oxide nanoparticles. The organic–inorganic hydrogels exhibit enhanced viscoelastic properties compared with analogous materials prepared using alkaline phosphatase.

Spontaneous molecular self-assembly into higher-ordered structures has been central to the design of novel organic and hybrid (organic/inorganic) nanostructured materials.[1] In particular, the design of bioactive building blocks, such as peptides with appropriate intermolecular recognition sites, has been exploited for the non-covalent self-assembly of 1-D bio-functionalized nanostructures.[2,3] Moreover, amphiphilicity of the building blocks can be tailored to facilitate entanglement of the 1-D nanostructures along with solvent entrapment to produce a wide range of viscoelastic hydrogels.[4,5] Although covalent cross-linking has been used to produce stabilized hydrogels, this method requires judicious control over the coupling reactions,[6] and alternative approaches based on supramolecular assembly have been explored.[4,5] Recent studies have shown that the concept of enzyme-directed assembly of small molecules can be extended to produce supramolecular hydrogels, for example based on the dephosphorylation of derivatized amino acids or peptides with fluorenyl- or naphthalene-functionalized end groups.[5] In many cases, the enzyme-mediated reaction results in an increase in the hydrophobicity of the gelator molecules, with the consequence that non-covalent intermolecular interactions such as hydrogen bonding and π stacking give rise to the reversible self-assembly of 3-D networks of entangled supramolecular nanofilaments. In a recent study, this approach was coupled with calcium phosphate mineralization to produce supramolecular hydrogels with integrated hybrid components.[7]

Although enzymes demonstrate excellent substrate specificity, their potential as agents in materials science is often hindered by their structural and functional fragility, lack of long-term stability under processing conditions, and difficulties in recovery and/or recycling. On the other hand, metal and metal oxide nanoparticles display size-dependant catalytic properties, chemical robustness and extended stability, suggesting that under certain conditions inorganic nanoparticles could be used to mimic aspects of biological functions related to specific enzymes. For instance, there are a growing number of examples in which Fe_3O_4, Co_3O_4, FeS, Au, Au@Pt, $CoFe_2O_4$ and V_2O_5 nanoparticles have been shown to exhibit peroxidase-like activity.[8] Specifically, cerium oxide nanoparticles and various lanthanide ions and/or their complexes have been employed to mimic alkaline phosphatase functions involved in the dephosphorylation of small organic molecules, nucleotides and peptides.[9] However, application of metal oxide nanoparticles to trigger the self-assembly of small molecules into supramolecular hydrogels remains unexplored. Herein, we demonstrate for the first time to our knowledge a facile method in which the intrinsic alkaline phosphatase-like activity of cerium oxide nanoparticles is exploited for the dephosphorylation of *N*- fluorenylmethyloxycarbonyl tyrosine-(*O*)-phosphate (FMOC-Tyr-P) (Scheme 1 ESI†). As a consequence, the hydrolysis reaction converts a charged amino acid derivative into a hydrogelator species (FMOC-Tyr) of lower charge, which subsequently self-associates to form a viscoelastic hydrogel comprising supramolecular nanofilaments and entrapped cerium oxide nanoparticles.

Nanoparticle-containing supramolecular hydrogels were prepared by adding 100 μL of aqueous FMOC-Tyr-P in alkaline buffer (50 mM Tris-HCl, 50 mM Na_2CO_3, 1 mM $MgCl_2$, pH 10.2) to 100 μL of an aqueous dispersion of well-crystalline cerium oxide nanoparticles (0.3 g mL^{-1}, pH 8.5, fluorite, Rhodia, Fig. S1, ESI†), and leaving the mixture (with final substrate concentrations of 50, 25, 12.5 or 8.3 mM) to stand at room temperature in the dark for 24 h. The resulting yellow-coloured hydrogels (pH 7.8) were semi-transparent and showed no gravity-induced flow upon inversion of the sample vial (Fig. 1a). Transmission electron microscopy (TEM) images of unstained samples of the hydrogels (Fig. 1b and c, and Fig. S2, ESI†) and tapping mode atomic force microscopy (AFM) studies (Fig. S3, ESI†) showed a continuum of cerium oxide nanoparticles that were penetrated by a semi-rigid and entangled matrix of flat ribbon-like helical nanofilaments, which were several micrometers long and 10–20 nm in width. High resolution TEM and energy dispersive elemental analysis further confirmed that the cerium nanoparticles were present along the seam of the

Centre for Organized Matter Chemistry, School of Chemistry, University of Bristol, Bristol, BS8 1TS, UK.
E-mail: avinash.patil@bristol.ac.uk, s.mann@bristol.ac.uk;
Fax: 0044-117-9290509; Tel: 0044-117-3317215

† Electronic supplementary information (ESI): Structural data for cerium oxide nanoparticles, TEM, AFM images of hydrogel nanofilaments, and NMR spectroscopy data are provided. DOI: 10.1039/c2cc33351a

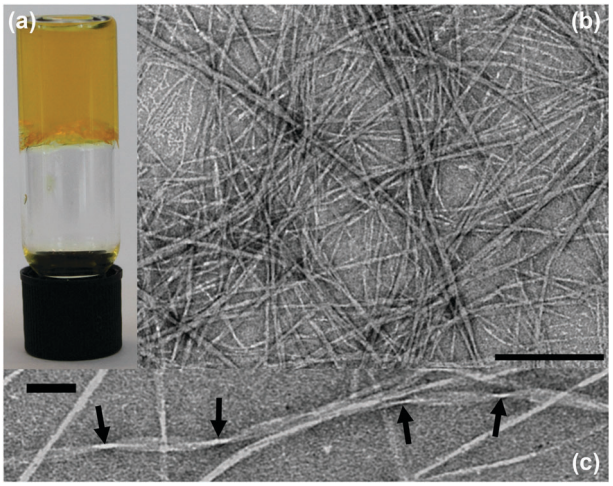

Fig. 1 (a) Photograph showing self-supported supramolecular hydrogel produced by cerium oxide nanoparticle-mediated dephosphorylation of FMOC-Tyr-P (50 mM). (b,c) Unstained TEM micrographs of corresponding FMOC-Tyr hydrogel network of semi-rigid nanofilaments (b), and high magnification image showing ribbon-like helical morphology (arrows) of individual nanofilaments (c). Scale bars; (b) 500 nm, and (c) 100 nm.

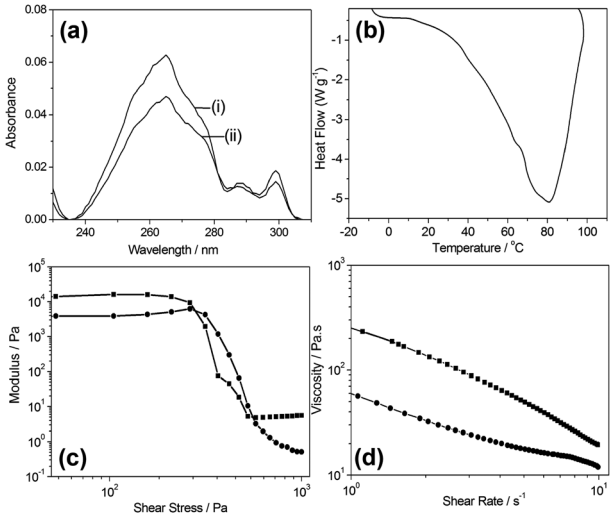

Fig. 2 (a) UV-vis spectra of aqueous FMOC-Tyr-P (i), and corresponding FMOC-Tyr hydrogel (ii) produced in the presence of cerium oxide nanoparticles, (Note: The broad absorption spectrum of the hydrogel masks the peak at 290 nm corresponding to cerium oxide nanoparticles) (Fig. S8, ESI†) (ii). (b) DSC thermogram of hydrogel prepared from 50 mM FMOC-Tyr-P showing broad gel to sol transition centred at 80 °C. (c) Oscillatory amplitude sweeps at a constant frequency of 1 Hz for hydrogel prepared at 50 mM FMOC-Tyr-P showing linear viscoelastic region for the storage (G′, ■) and loss (G″, ●) moduli (d) Viscosity profiles of cerium oxide nanoparticle-catalysed hydrogels prepared at 50 mM (■) or 25 mM (●) FMOC-Tyr-P concentrations.

nanofilaments (Fig. S4, ESI†). Control solutions involving mixtures of buffer and aqueous dispersions of cerium oxide nanoparticles remained fluid, confirming that self-assembly of the small-molecule amino acid derivative was responsible for hydrogelation.

Cerium oxide-mediated dephosphorylation of FMOC-Tyr-P was confirmed using ^{13}C and ^{31}P NMR spectroscopy. The ^{31}P NMR spectrum of FMOC-Tyr-P gave a resonance at −11.64 ppm corresponding to the phosphate ester group that was absent in the hydrogel samples, which showed a new peak at 0.17 ppm assigned to inorganic phosphate (Fig. S5, ESI†). Similarly, the resonance at 142.4 ppm associated with C–O–P(O)$(OH)_2$ in the ^{13}C NMR spectrum of FMOC-Tyr-P disappeared and was replaced in the hydrogel spectra by a peak corresponding to C–OH at 152.1 ppm (Fig. S6,S7, ESI†). These observations indicated that cerium oxide was an effective catalyst for phosphate ester bond hydrolysis of FMOC-Tyr-P, and that supramolecular self-assembly of dephosphorylated FMOC-Tyr molecules occurred readily in the presence of the inorganic nanoparticles.

The structural and physical properties of the as-prepared FMOC-Tyr/nanoparticle hydrogels were investigated by several methods. UV-vis spectra of the hydrogels showed three characteristic absorption peaks corresponding to π–π*, n-π* and n-π* transitions, at 265, 288 and 299 nm, respectively. Significantly, the hydrogel samples exhibited characteristic hypochromicity, as evidenced by changes in the absorption intensity ratios (A_{265}/A_{299}) from a value of 3.5 : 1 for aqueous FMOC-Tyr-P to 3.2 : 1 for the hydrogels (Fig. 2a). This was consistent with the presence of stacking interactions between fluorenyl moieties associated with fibril formation.[5d] DSC thermograms of the nanoparticle-containing hydrogels showed a broad endothermic peak in the region of 75–80 °C, corresponding to a reversible gel–sol melting transition. Oscillatory amplitude sweeps at a constant frequency of 1 Hz of hydrogels prepared using 50 mM FMOC-Tyr-P solutions and aged for 1 day showed typical supramolecular hydrogel behaviour within the linear viscoelastic region with almost parallel storage (elastic) G′ and loss (viscous) G″ moduli up to a shear stress of 570 Pa (Fig. 2c). The two cross-over points observed in the oscillatory amplitude sweep could be attributed to structural deformation resulting in a severely dehydrated nanofilamentous network. The three-fold increase seen in the elastic modulus compared to the viscous modulus was consistent with a persistent semi-rigid gel network, and indicative of solid-like viscoelastic behaviour. Cerium oxide-containing hydrogels prepared at lower FMOC-Tyr-P concentrations (25 mM) showed similar solid-like viscoelastic properties but exhibited structural deformation at a much lower shear stress value of 63 Pa (Fig. S9, ESI†). These observations were consistent with the viscometry measurements, which showed an increase in the viscosity values with increasing FMOC-Tyr-P concentration (Fig. 2d). Typically, at very low shear rates, the viscosities were 252 and 60 Pa.s for nanoparticle-containing hydrogels prepared from 50 and 25 mM FMOC-Tyr-P, respectively.

Cross-polarized optical microscopy images of cerium oxide-containing hydrogels prepared at a FMOC-Tyr-P concentration of 50 mM revealed 100–150 μm-sized domains displaying Maltese cross patterns (Fig. 3a), whereas at 25 mM anisotropic domains with nematic birefringence (Fig. 3b) were observed, both of which were dispersed in an isotropic phase. The Maltese cross patterns exhibited a strong blue fluorescence in the presence of the dye Hoechst 3325 (Fig. S10a, ESI†), indicative of spherulites comprising radially ordered nanofilaments with a well-defined, π-stacked FMOC-Tyr superstructure.[10,11] This was consistent with environmental scanning electron

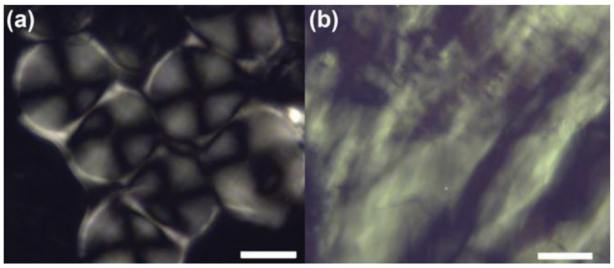

Fig. 3 Cross-polarized optical microscopy images of hydrogels prepared by cerium oxide nanoparticle-mediated dephosphorylation of FMOC-Tyr-P at concentrations of 50 mM (a) and 25 mM (b), showing the presence of Maltese cross patterns (spherulites) or nematic birefringence, respectively. Scale bar = 100 μm.

microscopy (ESEM) micrographs, which indicated that the Maltese cross structures corresponded to discrete spheroidal 100–120 μm-sized particle-like domains (Fig. S10b, ESI†). Although the differences in texture were attributed primarily to changes in FMOC-Tyr-P concentration, the possibility that nucleation of the FMOC-Tyr nanofilaments occurred specifically on the surface of the cerium oxide nanoparticles could not be ruled out.

In summary, we have shown that cerium oxide nanoparticles are capable of alkaline phosphatase-like activity, with the consequence that viscoelastic, amino acid-based supramolecular hydrogels comprising an entangled network of helical ribbon-like nanofilaments and inorganic nanoparticles can be produced by abiogenic catalysis-mediated self-assembly. The nanoparticle-containing FMOC-Tyr hydrogels were responsive to external stimuli such as temperature or mechanical forces, with the consequence that they could be reversibly assembled and disassembled by melting or shear thinning of the supramolecular structure. The catalytic dephosphorylation behaviour of the cerium oxide nanoparticles was attributed to the Lewis acidity associated with Ce^{3+}/Ce^{4+} surface sites that are capable of not only coordinating phosphoryl oxygens but also reducing the activation energy of P–O bond scission by facilitating nucleophilic attack from neighbouring surface-bound hydroxyl groups.[9] Although mechanistically different, the results indicate that cerium oxide nanoparticles can be used as plausible mimics of enzymatic transformations involving peptide dephosphorylation and coupled supramolecular self-assembly.[6] However, we noted several differences between the physical properties of the nanoparticle-containing hydrogels and their FMOC-Tyr counterparts prepared by enzyme-mediated self-assembly under comparable conditions. For example, use of the cerium oxide nanoparticle catalyst (0.3 g mL^{-1}) produced hydrogels from FMOC-Tyr-P concentrations as low as 8.3 mM (Fig. S2, ESI†), while a limiting amino acid concentration of *ca.* 50 mM was required in the presence of alkaline phosphatase. Moreover, alkaline phosphatase-mediated hydrogels were softer, less viscous, and displayed a considerable degree of structural deformation at much lower shear stress values (10 Pa),[5d] compared with hydrogels prepared in the presence of cerium oxide nanoparticles. The increase in mechanical strength was attributed primarily to the nanoparticle-mediated self-assembly of a semi-rigid matrix of supramolecular filaments, which become entangled to produce a robust hydrogel comprising spherulitic/nematic domains, and exhibiting a gel–sol transition temperature (75–80 °C) approximately 40 °C higher than that observed for enzyme-mediated FMOC-Tyr hydrogels.[5d] Entrapment of the cerium oxide nanoparticles within the gel network could also contribute towards the increased stiffness and viscosity.

Finally, the use of cerium oxide and other inorganic nanoparticles[9] in the catalytic dephosphorylation of biologically active amino acids and peptides could have general relevance in developing supramolecular hydrogels with hybrid structures and functions. In this regard, we note that several recent studies have demonstrated promising biomedical applications based on cerium oxide nanoparticles,[12] suggesting that embedding inorganic nano-catalysts of this type within small-biomolecule hydrogels could represent an important step towards novel forms of soft, bioactive materials.

The authors thank the University of Bristol, UK for financial support, Dr Andrew Collins, Jonathan A. Jones, Judith Mantell (Wolfson Bioimaging Facility, University of Bristol), Prof. Tony Miles and Dr Phil Pollintine (University of Bath) for assistance with AFM, HRTEM, ESEM and rheology measurements respectively.

Notes and references

1 (*a*) S. Mann, *Nat. Mater.*, 2009, **8**, 781; (*b*) S. Stupp, *Chem. Rev.*, 2005, **105**, 1023.
2 R. V. Ulijn and D. N. Woolfson, *Chem. Soc. Rev.*, 2010, **39**, 3349.
3 (*a*) J. B. Matson and S. I. Stupp, *Chem. Commun.*, 2012, **48**, 26; (*b*) M. Zezler and R. V. Ulijn, *Chem. Soc. Rev.*, 2010, **39**, 3351.
4 (*a*) R. V. Ulijn, *J. Mater. Chem.*, 2006, **16**, 2217; (*b*) Z. Yang, G. Liang and B. Xu, *Acc. Chem. Res.*, 2008, **41**, 315; (*c*) M. E. Hahn and N. C. Gianneschi, *Chem. Commun.*, 2011, **47**, 11814; (*d*) D. J. Adams, *Macromol. Biosci.*, 2011, **11**, 160; (*e*) J. Dash, A. J. Patil, R. N. Das, F. L. Dowdall and S. Mann, *Soft Matter*, 2011, **7**, 8120.
5 (*a*) Z. Yang, H. Gu, D. Fu, P. Gao, J. K. Lam and B. Xu, *Adv. Mater.*, 2004, **16**, 1440; (*b*) S. Toledano, R. J. Williams, V. Jayawarna and R. V. Uljin, *J. Am. Chem. Soc.*, 2006, **128**, 1070; (*c*) A. K. Das, R. Collins and R. V. Ulijn, *Small*, 2008, **4**, 279; (*d*) R. Krishna Kumar, X. Yu, A. J. Patil, M. Li and S. Mann, *Angew. Chem., Int. Ed.*, 2011, **50**, 9343.
6 (*a*) T. Vermonden, R. Censi and W. E. Hennink, *Chem. Rev.*, 2012, DOI: 10.1021/cr200157d; (*b*) K. Y. Lee and D. J. Mooney, *Chem. Rev.*, 2001, **101**, 1869.
7 Z. A. C. Schnepp, R. Gonzalez-McQuire and S. Mann, *Adv. Mater.*, 2006, **18**, 1869.
8 (*a*) L. Gao, J. Zhuang, L. Nie, J. Zhang, Y. Zhang, N. Gu, T. Wang, J. Feng, D. Yang, S. Perrett and X. Yan, *Nat. Nanotechnol.*, 2007, **2**, 577; (*b*) Z. Dai, S. Liu, J. Bao and H. Ju, *Chem.–Eur. J.*, 2009, **15**, 4321; (*c*) W. He, Y. Liu, J. Yuan, J. J. Yin, X. Wu, X. Hu, K. Zhang, J. Liu, C. Chen, Y. Ji and Y. Guo, *Biomaterials*, 2011, **32**, 1139; (*d*) Y. Jv, B. Li and R. Cao, *Chem. Commun.*, 2010, **46**, 8017; (*e*) R. Andre, F. Natalio, M. Humanes, J. Leppin, K. Heinze, R. Wever, H. C. Schroder, W. E. G. Muller and W. Tremel, *Adv. Funct. Mater.*, 2010, **21**, 501; (*f*) W. Shi, X. Zhang, S. He and Y. Huang, *Chem. Commun.*, 2011, **47**, 10785; (*g*) J. Mu, Y. Wang, M. Zhao and L. Zhang, *Chem. Commun.*, 2012, **48**, 2540.
9 (*a*) F. Tan, Y. Zhang, J. Wang, J. Wei, Y. Cai and X. Qian, *J. Mass Spectrom.*, 2008, **43**, 628; (*b*) M. H. Kuchma, C. B. Komanski, J. Colon, A. Teblum, A. E. Masunov, B. Alvarado, S. Babu, S. Seal, J. Summy and C. H. Baker, *Nanomed.: Nanotechnol., Biol. Med.*, 2010, **6**, 738; (*c*) G. Cheng, J.-L. Zhang, Y.-L. Liu, D.-H. Sun and J.-Z. Ni, *Chem. Commun.*, 2011, **47**, 5732; (*d*) N. W. Luedtke and A. Schpartz, *Chem. Commun.*, 2005, 5426.
10 A. Aggeli, M. Bell, L. M. Carric, C. W. G. Fishwick, R. Harding, P. J. Mawer, S. E. Radford, A. E. Strong and N. Boden, *J. Am. Chem. Soc.*, 2003, **125**, 9619.
11 M. R. H. Krebs, C. E. MacPhee, A. F. Miller, I. E. Dunlop, C. M. Dobson and A. M. Donald, *Proc. Natl. Acad. Sci. U. S. A.*, 2004, **101**, 14420.
12 I. Cleardo, J. Z. Pedersen, E. Traversa and L. Ghibelli, *Nanoscale*, 2011, **3**, 1411.

